A simplified method to interpret the mechanism of drug release from thin polymeric films by drug diffusivity measurements

International Journal of Pharmaceutics 675 (2025) 125491

Contents lists available at ScienceDirect

International Journal of Pharmaceutics

journal homepage: www.elsevier.com/locate/ijpharm

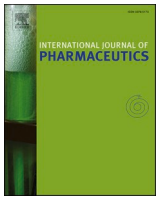

A simplified method to interpret the mechanism of drug release from thin polymeric films by drug diffusivity measurements

Karin Korelc [a,*], Martina M. Tzanova [a,b], Anette Larsson [c], Mario Grassi [d], Massimiliano Pio Di Cagno [a,e,1], Ingunn Tho [a,1]

[a] Department of Pharmacy, Faculty of Mathematics and Natural Sciences, University of Oslo, Sem Sælands vei 3, 0371 Oslo, Norway
[b] Department of Life Sciences and Health, Faculty of Health Sciences, Oslo Metropolitan University, Oslo, Norway
[c] Dept. of Chemistry and Chemical Engineering, Chalmers University of Technology, Gothenburg, Sweden
[d] Department of Engineering and Architecture, University of Trieste, Via Alfonso Valerio, 6/1, 34127 Trieste, Italy
[e] Department of Chemical and Pharmaceutical Sciences, University of Trieste, Via L. Giorgieri 1 – 34127 Trieste, Italy

ARTICLE INFO

Keywords:
Drug-polymer affinity
UV–Vis localized spectroscopy
Data-fitting
Film formulations
Modified drug release
Copolymers
Poly(vinyl alcohol-co-vinyl acetate)

ABSTRACT

Drug-polymer interactions and their respective affinities provide vital information for developing any polymer-containing drug delivery system, such as oral films. This paper offers a simplified method to estimate the effects of interactions between the drug and polymers in corresponding film formulations using a recently developed Fickian diffusion-based methodology. Poly(vinyl alcohol-co-vinyl acetate) (PVA/PVAc) copolymers were used as film matrix formers. To systematically vary the hydrophilicity of the polymer and drug, PVA/PVAc copolymers (monomer ratios 35:65, 50:50, 74:26, 88:12, 98:2) and model drugs, hydrochlorothiazide and caffeine (with a factor 1:30 in solubility) were used. Drug diffusivities determined in a polymer solution (5 % w/v) were compared to classical in vitro drug release from the films. The drug release rate from films containing copolymers with a lower VA/VAc ratio (35:65, 50:50, and 74:26) was significantly different for the two drugs in the first 30 min. It was found that this diffusivity method provided valuable guidance in assessing drug-polymer affinity, described as the average theoretical partition constant $K_{m/w}$ between the polymer solution and pure aqueous media. This partition constant could be correlated to the drug release rate and serve as a simple, easy, and inexpensive screening method to provide deeper mechanistic insight into drug release mechanisms. This would allow enhanced sustainability and accelerate the formulation development process by reducing resources needed for the development of film formulations.

1. Introduction

Polymers are among the most frequently used excipients in drug delivery systems (DDS). In thin film formulations, the matrix is composed of a polymer with or without plasticizers. A wide range of film-manufacturing technologies and a variety of polymers to choose from have enabled the development and increased popularity of films as solid dosage forms. Polymer choice is crucial as it will govern the product characteristics, e.g. drug release rate, mucoadhesion, and mechanical properties (Karki et al., 2016). The drug-polymer interaction will play an important role in drug delivery, as it may affect drug dissolution and drug release (Puttipipatkhachorn et al., 2001). Studies of drug-polymer interactions often require methods with several preparation steps, such as Fourier-transform infrared spectroscopy (FT-IR), Raman spectroscopy, differential scanning calorimetry (DSC), and X-ray powder diffraction (XRPD) (Medarević et al., 2019).

The hydration and drug release processes from thin hydrophilic film formulations can be suggested to resemble, to some extent, the processes involved in drug release from hydrophilic matrix tablets. The first step for these systems is hydration, where water penetrates into the formulation. This results in a decrease in the glass transition temperature (T_g), a transition of the polymers from a glassy to a rubbery state, and the creation of a locally increased osmotic pressure that facilitates even more water transport into the formulation, leading to the dissolution of the polymer and formation of an entangled polymer solution. At the same time, the solid drug particles start to dissolve in the hydrated

* Corresponding author at: Sem Sælands vei 3, 0371 Oslo, Norway.
E-mail address: karin.korelc@farmasi.uio.no (K. Korelc).
[1] Shared last-authorship (equal contribution to this work).

https://doi.org/10.1016/j.ijpharm.2025.125491
Received 6 February 2025; Received in revised form 14 March 2025; Accepted 15 March 2025
Available online 26 March 2025

entangled polymer solution and diffuse out from the solution (Colombo, 1993). During this diffusion process, the presence of polymer chains may physically hinder the drug molecules, and drug-polymer interactions may occur. The net transport time for the drug depends on all these processes simultaneously. Classically, the drug release rate from the hydrated entangled polymer layer is modeled using Fick's second law of diffusion (explained in section 2.3.).

In vitro drug release studies from films often use diffusion cells (e.g., Franz diffusion cells) or more specialized devices such as the microfluidic flow-through cell (Adrover et al., 2018; Adrover & Nobili, 2015). These methods can be time-consuming, require large volumes of liquids, and suffer from high variability, making them unsuitable for early-stage drug development and formulation screening purposes (Desmedt et al., 2015; Pulsoni et al., 2022).

Recently, various poly(vinyl alcohol-co-vinyl acetate) (PVA/PVAc) copolymers were explored as film formers in oral films (Korelc et al., 2024). These are commercially available synthetic copolymers composed of hydrophilic vinyl alcohol (VA) and hydrophobic vinyl acetate (VAc) monomers (Fig. 1a and b) with varying ratios between the monomer units. The copolymer structure (dictated by their composition) affects their physicochemical properties, e.g. hydrophilicity, water solubility, crystallinity, and disintegration (Atanase & Riess, 2010). The copolymers used in this work have partial block-wise distributions (Korelc et al., 2024), which can result in the formation of highly hydrophobic regions in the presence of a higher proportion of VAc chains. This allows polymer chains to form different types of inter- and intramolecular interactions, such as hydrophobic interactions, hydrogen bonds, and/or van der Waals interactions. PVA/PVAc copolymers with a higher proportion of hydrophobic VAc chains are expected to form hydrophobic interactions with drug molecules of a more hydrophobic character, such as hydrochlorothiazide, potentially resulting in a slower and uncomplete drug release from the system. Smaller and hydrophilic drug molecules, such as caffeine, are surrounded by water molecules with which they can form hydrogen bonds, and the likelihood of interacting with the polymer is therefore smaller.

This work explores the possibility of predicting drug release from hydrated films by microscopic diffusivity investigations. In 2018, Di Cagno *et al.* introduced the UV–Vis localized spectroscopy approach (Di Cagno et al., 2018). This spectroscopic method was initially developed to estimate drug diffusivity in solutions and from nanocarrier-based formulations (Di Cagno et al., 2018; Di Cagno & Stein, 2019; Tzanova et al., 2022). It is based on the collection of time-resolved concentrations of released drug in an unstirred environment, which is fitted by mathematical models derived from Fick's second law of diffusion to extract the parameters of interest such as diffusivities and partitions coefficients. Fig. 2 qualitatively illustrates the drug concentration profile

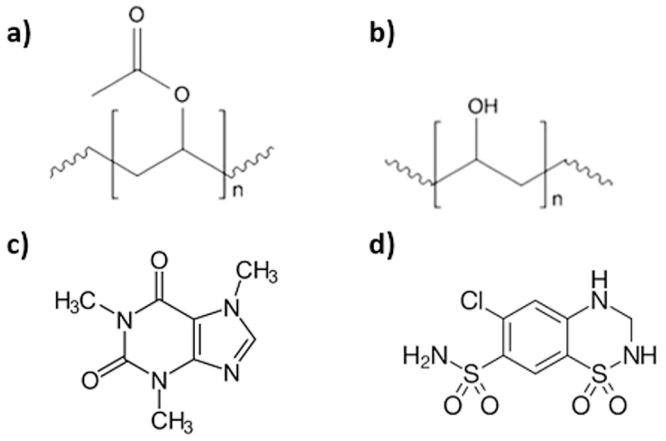

Fig. 1. The structure of a) poly(vinyl acetate), b) poly(vinyl alcohol), c) caffeine and d) hydrochlorothiazide.

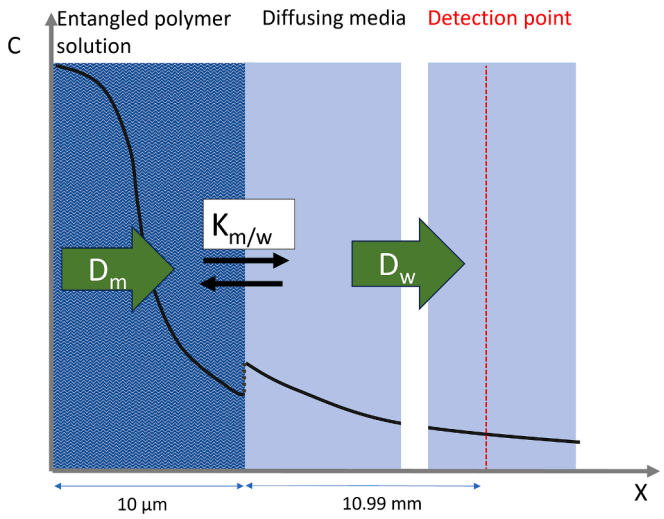

Fig. 2. A schematic illustration of a momentary snapshot of the physical model applied in this work describes the drug release from a polymer solution into a cuvette filled with water, which should resemble the release from a hydrated film. Drug molecules diffuse through the hydrated film following a concentration (c) gradient of free drug (black line) and according to the diffusivity of the drug in the polymer solution (D_{eff}, here marked as D_m). Drug molecules are moving from one phase (polymer solution) into the other phase (water). This process is controlled by the partition coefficient between the two phases, i.e., the polymer solution and water ($K_{m/w}$). Lastly, drug molecules will diffuse through the water according to the diffusivity of the drug in water (D_w). X represents the distance from the bottom of the cuvette. The detection point is marked with a red line.

at a momentary snapshot, occurring in our experimental set-up. In permeation studies, Falavigna *et al.* utilized the same empirical approach to give a magnitude to the mucus layer as an additional permeation barrier (Falavigna et al., 2020). Mucin, being a glycoprotein, swells in an aqueous environment and creates a viscous barrier, which in vivo lubricates and protects mucosal surfaces and works as a barrier for drug permeation. They studied mucus layers consisting of 0.1–0.6 % (w/v) porcine stomach mucin (type III) in PBS (pH 7.4). The effective diffusivity (relative diffusivity) was estimated for four chemically diverse compounds, and a negative effect of mucus on drug diffusivity was demonstrated for all compounds (to a varying degree) (Falavigna et al., 2020).

The aim of this work was to verify if the localized UV–Vis spectroscopy method developed by Di Cagno *et al.* was suited to screen drug-polymer affinity and predict release behavior in thin films composed of PVA/PVAc copolymers with different monomer ratios and drugs with different solubility properties in a simple and fast manner. The drug diffusivity parameters were determined for a water-soluble drug, caffeine (CAF), and a poorly water-soluble drug, hydrochlorothiazide (HCT) (Fig. 1c and d), dissolved in film-forming PVA/PVAc copolymers with different monomer ratios (35:65, 50:50, 74:26, 88:12, 98:2). We hypothesized that this method could be used to predict drug-polymer interactions and release from films and that the drug with lower water solubility will have a higher affinity for the copolymers with a higher acetate proportion, contributing to slower drug release from films. A mathematical model was used to interpret the experimental data, and release studies were performed on corresponding thin films to evaluate the method's suitability for film formulation development.

2. Materials and methods

2.1. Materials

HCT and CAF were provided by Sigma Aldrich (St. Louis, MO, USA).

PVA/PVAc copolymers were obtained from Kuraray Poval™ (Frankfurt, DE). All solutions were prepared with Milli-Q (mQ) water purified using a purification system for ultrapure water (Merck, Darmstadt, DE). $NaH_2PO_4 \times 2\ H_2O$ was obtained from VWR Chemicals (Radnor, PA, USA). $Na_2HPO_4 \times 2\ H_2O$ was purchased from Merck (Darmstadt, DE). NaOH pellets were purchased from Sigma-Aldrich (Steinheim, DE).

2.2. Methods

2.2.1. Solubility study

Solubility studies were performed for HCT and CAF by adding an excess amount of drug to mQ water and stirring the suspensions at 300 rpm for 72 h at room temperature (RT) (approx. 23 °C) in triplicates. Afterward, the suspension was filtered (0.2 μm), diluted as necessary, and the amount of dissolved drug was quantified using a Spectramax 190 microplate reader (Molecular Devices LLC, Sunnyvale, CA, USA) at the wavelength $\lambda = 273$ nm for HCT and CAF.

2.2.2. Intrinsic viscosity and critical overlap concentration

Intrinsic viscosity (η) and critical overlap concentration (c*) for the copolymers were determined using Micro-Ostwald Viscometer (type 516 10: Capillary No. I, Constant K = 0.01, SI Analytics, DE). The polymers were dispersed in mQ water at 4–5 concentrations per copolymer. 2 mL of the dispersion was added to the Ostwald Viscometer, which was placed into the thermostatic water at the temperature of 25.1 ± 0.1 °C, and the sample was equilibrated for 5 min. The flow time (t) between two marked points was automatically recorded. Triplicates were performed for each polymer concentration, and each measurement was performed 3 times per sample. The flow time for the background (mQ water) (t_0) was recorded. Relative viscosity (η_r), specific viscosity (η_{sp}), and reduced viscosity (η_{red}) were calculated as shown in Eq. (1), Eq. (2), and Eq. (3), respectively.

$$\eta_r = \frac{t}{t_0} \tag{1}$$

$$\eta_{sp} = \eta_r - 1 \tag{2}$$

$$\eta_{red} = \frac{\eta_{sp}}{c} \tag{3}$$

The intrinsic viscosity (η) was obtained by plotting the reduced viscosity against concentration and extrapolating η_r to $c_0 = 0$. The critical overlap concentration was estimated as $c^* = 1.22/\eta$ by combining information from Amsden (Amsden, 2022) with the gyration radius (Rg) from Flory (Flory, 1953).

The polymers were characterized with respect to molecular weight by size exclusion chromatography and degree of hydrolysis as well as block-distribution by ^{1}H NMR in an earlier study (Korelc et al., 2024).

2.2.3. Preparation of solutions for diffusion studies

Phosphate-buffered saline (PBS) 73 mM (pH 7.4) was prepared from $NaH_2PO_4 \times 2\ H_2O$ and $Na_2HPO_4 \times 2\ H_2O$ salts. The pH was adjusted to 7.4 using NaOH pellets, and osmolality was adjusted to 280–300 mOsm/kg by NaCl addition. The PBS was subsequently filtered through a 0.2 μm filter (Whatman® Nuclepore Track-Etch membrane filter; GE Healthcare Life Sciences, Maidstone, UK).

The polymer solutions were prepared by dispersing the polymer in mQ water (0.5 g/8 mL) and preparing a 250 μg/mL HCT/CAF solution in mQ water. 2 mL of the drug solution was added to the hydrated polymer to achieve a final concentration of 50 μg/mL drug and 50 mg/mL polymer (i.e., 5 % w/v polymer). The blank polymer samples were prepared by dispersing the appropriate amount of polymer (0.5 g) in 10 mL mQ water. The references used were HCT and CAF (50 μg/mL) dissolved in PBS to ensure a density difference between the drug solution and the water media. PBS was used as a solvent media for HCT and CAF to increase the density of the sample so that the injected sample could remain on the bottom of the cuvette after injection.

2.2.4. Viscosity

The viscosity of the polymer solutions was measured using the Brookfield viscometer DV2T (Middleboro, MA, USA) with the spindle CPA-40Z. The sample (500 μL) was measured at a temperature of 25 °C and a speed of 25 RPM using a 2-minute time point. The measurements were performed in triplicates.

2.2.5. Diffusion studies

The effects of PVA/PVAc copolymers on the diffusivity of two drugs with different physicochemical characteristics (Table 1) were studied using the method by Di Cagno *et al.* (Di Cagno et al., 2018). The experimental setup used semi-micro cuvettes with PTFE stopper ($V_{chamber} = 700$ μL, path length = 10 mm, Starna Scientific, Essex, UK), and the absorbance was determined using a double-array UV–Vis spectrophotometer UV-6300 PC (VWR International, PA, USA). Both the sample and reference cuvettes were filled with 675 μL mQ water. At time zero (t_0), 25 μL of the sample was injected into the bottom of the cuvette using a microneedle syringe (Hamilton Company, NV, USA) (Fig. 3). The measurements were performed at ambient conditions and at the wavelength $\lambda = 273$ nm (corresponding to their absorption maxima) for both HCT and CAF (Supplementary material, Fig. S1). The absorbance was recorded every 120 s for 20 h at 1.1 cm from the bottom of the cuvette (i.e., the origin of diffusion, X_0, see Fig. 3). This height has already been previously validated to be reliable for detecting small changes in diffusivity (Di Cagno et al., 2018). As a reference, absorbance for the polymer solution without the drug was measured at the same wavelength. The normalized drug absorbance was calculated by subtracting the absorbance value for the reference (polymer solution) from the absorbance for the drug-polymer formulations at each time point. Two replicates were used to determine the reproducibility, and the percentage of variation in concentration was calculated at each time point. The diffusion coefficient was obtained by mathematical model fitting to experimental data as detailed in Section 2.3. Furthermore, to evaluate the effect of polymer scattering and its impact on the UV–Vis curves, wavelength scans were conducted at various time points (from the start to 240 min) with and without HCT for the polymer with the highest scattering (PVA35).

2.2.6. Preparation of films

Films with CAF were prepared following the same methodology used for the HCT films previously described by us (Korelc et al., 2024). Briefly, 5 mg/mL CAF solution was prepared in ethanol:water (1:1) mixture. 8 g of polymer was dispersed in 20 mL of the solution to obtain a final polymer concentration of 40 % w/v and 5 mg/mL drug. Due to the poorer solubility of PVA98 in the solvent, half of the concentration of drug and polymer were used (20 % w/v and 2.5 mg/mL, respectively), keeping the same polymer-to-drug ratio in the films.

The films were printed using semi-solid extrusion (SSE) with Z-morph2 (Zmorph, Wroclaw, PL) using Autodesk Fusion 360 (Autodesk, San Rafael, CA, USA) to design a four-leaf clover shamrock and Voxelizer 2 (Zmorph, Wroclaw, PL) to control the printing parameters. The printing settings were as follows: layer height was set to 1 mm, and path width was 0.8 mm. Travel and printing speeds were 50 mm/s and 1.0 mm/s, respectively. The films were allowed to dry on the printing surface (Bench Surface protector, VWR International, FR) for 24 h before being stored in a desiccator box (room temperature, approx. 33 % relative humidity). The semi-solid extruded shamrock-shaped film pieces were about 3.9 cm × 3.9 cm in outer size, with each clover being consequently cut (approx. 2 cm^2) and considered a single dose. Each single-dose film piece contained 1.2 mg drug.

2.2.7. Drug release and film disintegration studies

The drug release studies were performed in the same way as for HCT films described in our previous work (Korelc et al., 2024). Briefly, approx. 100 mg film pieces (corresponding to single-dose, e.g. one

Table 1
Physicochemical properties of caffeine (CAF) and hydrochlorothiazide (HCT).

Drug	Mw (g/mol)	pKa	Charge (pH 7.4)	Log P	Log D	Water solubility (pH 7.0) (mg/mL)	λ_{max} (nm)	ε (cm^{-1} M^{-1})
CAF	194	14[a]	0	−0.07[a]	−0.07[b]	21.7[a]	273[c]	9123
HCT	298	7.9, 9.2[a]	0	−0.07[a]	n.a.	0.72[a]	273	18033

[a] : obtained from www.pubchem.ncbi.nlm.nih.gov (*PubChem*, n.d.).
[b] : obtained from (Benet et al., 2011).
[c] : obtained from Bhawani et al. (Ahmad Bhawani et al., 2015). n.a. = not applicable.

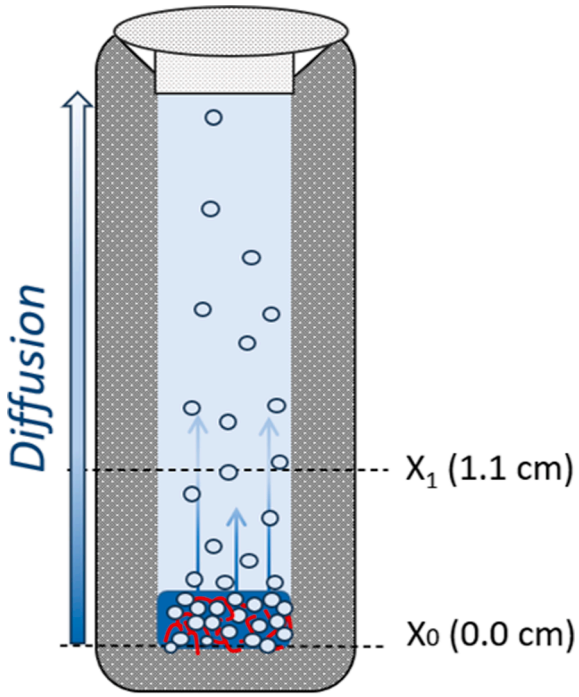

Fig. 3. Schematic illustration of the diffusional model and height points. X_0 is the bottom point (the sample injection point), and X_1 is the measurement point (1.1 cm). The dots represent the diffusion of drug molecules, and the red coils represent the polymer chains.

clover of a shamrock with a drug loading of 1.2 mg) were added to the dissolution media (10 mL of 0.01 M PBS with pH 7.4) to ensure sink conditions. The samples were put into Environmental Shaker-Incubator (Biosan, Riga, LV) and shaken at 100 rpm at the temperature of 30 °C. 150 µL samples were withdrawn at the following time points: 2, 5, 10, 15, 20, 25, 30, 45, 60, 90, 120, 180 and 240 min, and the withdrawn volume was replaced with fresh pre-heated PBS. The films were visually inspected throughout the drug release study for disintegration and behavior in the release media. The samples were diluted with PBS as necessary and filtered using a 0.2 µm filter before quantification. The data for HCT films were obtained from our recent paper (Korelc et al., 2023).

CAF was quantified using reversed-phase HPLC-UV using the Nova-pak® C18 (4 µm; 3.9 x 150 mm) column. The mobile phase consisted of water:methanol in a 70:30 ratio, using isocratic elution with a flow rate of 1.0 mL/min. The column oven temperature was set to 25 °C and the injection volume of the sample was 10 µL. The total run time was 5 min, with the caffeine retention time at 2.55 min. Detection was performed at the wavelength $\lambda = 273$ nm. The HPLC-UV method was checked for linearity, limit of detection (LOD), and limit of quantification (LOQ). The results were normalized to 100 mg film pieces to directly compare the samples.

2.3. Mathematical model

The description of drug transport in our diffusional apparatus can be challenging because of the concurrence of different phenomena. Due to the existence of concentration gradients, the polymeric chains of the polymer solution could diffuse in the upper mQ water phase, and, symmetrically, water molecules of the mQ water phase could diffuse in the lower polymer solution (see Fig. 3). Thus, polymer concentration in the two phases would be time-dependent, and the interface position between the two phases would be not well defined. Additionally, drug diffusion in the polymer solution could be affected by drug-polymer interactions as only drug molecules that are not bound to the polymeric chains can freely diffuse (free drug), while bound drug molecules cannot diffuse. Relying on our experimental data, we can affirm that the diffusion of the polymeric chains into the mQ water phase is limited within our experimental time (see section 2.2.5). Assuming that possible drug interaction phenomena with polymeric chains (absorption and desorption) are very fast in comparison to drug diffusion, we can assume that the free and bound drug fractions are in thermodynamic equilibrium. Consequently, the drug diffusion process in the polymer solution can be described by Fick's law with a concentration-dependent diffusion coefficient (effective diffusion coefficient, D_{eff}) (Grassi et al., 2006).

$$\frac{\partial C_{ps}}{\partial t} = \left(\frac{\partial}{\partial x}\left(D_{eff}\frac{\partial C_{ps}}{\partial x}\right)\right) \tag{4}$$

where t is time, x is the axial coordinate and C_{ps} is the drug concentration in the polymer solution. Supposing that the drug concentration in the polymer solution is much smaller than drug solubility, D_{eff} becomes constant and is related to the free drug diffusion coefficient (D_m) inside the polymer solution through the polymer solution/mQ water partition coefficient ($K_{m/w}$) (Amsden, 2022):

$$D_{eff} = \frac{D_m}{K_{m/w}} \tag{5}$$

It is important to remember that, in our simplifying hypotheses, $K_{m/w}$ is equal to $(1 + k_a/k_d)$ where k_a and k_d are, respectively, the drug adsorption and desorption constants of polymeric chains (Amsden, 2022). The drug diffusion inside the upper aqueous environment (upper cuvette part, see Fig. 2) can be accounted for by the classical Fick's second law:

$$\frac{\partial C_w}{\partial t} = \left(\frac{\partial}{\partial x}\left(D\frac{\partial C_w}{\partial x}\right)\right) \tag{6}$$

where C_w and D are, respectively, drug concentration and diffusion coefficient within the mQ water phase.

Solutions to Eq. (4) and Eq. (6) were found considering the following initial and boundary conditions:

Initial conditions:

$$C_{ps} = C_0 \qquad 0 \le x \le x_1 \tag{7}$$

$$C_w = 0 \qquad x_1 < x \le L \tag{8}$$

Boundary conditions:

$$\left.\frac{\partial C_{ps}}{\partial x}\right|_{x=0} = 0 \quad (9)$$

$$\left.\frac{\partial C_{w}}{\partial x}\right|_{x=L} = 0 \quad (10)$$

$$D_{eff}\left.\frac{\partial C_{ps}}{\partial x}\right|_{x=x_1} = D\left.\frac{\partial C_{w}}{\partial x}\right|_{x=x_1} \quad (11)$$

$$C_{ps}|_{x=x_1} = K_{m/w}C_{w}|_{x=x_1} \quad (12)$$

where L is the cuvette thickness. Initial conditions (Eq. (7) and Eq. (8) state that, at the beginning (t_0), the drug is uniformly distributed in the polymer solution at concentration C_0 while the upper aqueous phase does not contain the drug. Boundary conditions ensure that the drug cannot cross either the cuvette bottom (impermeable wall in x = 0; Eq 0.9) nor the cuvette top (impermeable wall in x = L; Eq. (10). In addition, Eq. (11) ensures that there is no drug accumulation at the polymer solution/mQ water interface, i.e. the drug flux leaving the polymer solution is equal to the drug flux entering the mQ water phase. Finally, thermodynamic equilibrium conditions were supposed to be obtained at the polymer solution/aqueous interface (Eq. (12), implying that the drug concentration on the two interface sides can be different (see Fig. 2).

Unfortunately, as D differs from D_{eff}, it is not possible to get a model analytical solution. Accordingly, Eq. (4) and Eq. (6) have been numerically solved according to the control volume method (Patankar, 1980) by building a proper Microsoft Excel user-defined function. In order to ensure the numerical solution reliability, the polymer solution and the water phases were subdivided into 10 and 100 parts, respectively. Model fitting parameters were D_{eff} and $K_{m/w}$. D was evaluated according to the Stokes-Einstein (the estimated molecular radius, r_s, for CAF is 2.82 Å and for HCT is 2.80 Å).

Both the χ^2 test as well as the F-test were performed as statistical analyses to evaluate both the variance between experimental and mathematical data (χ^2 test) and the significance of the variances of the experimental data and fitting data sets (F-test).

3. Results and discussion

HCT and CAF were used as model drugs to explore the affinity of drugs to polymers with different physicochemical properties and release from films made from five PVA/PVAc copolymers with varying monomer ratios. The polymers have previously been shown to have a molecular weight of approximately 23–24 kDa (the most hydrophobic types could not be analyzed) and display block-wise distribution of the PVA and PVAc segments (Korelc et al., 2024). The degree of hydrolysis was confirmed to be in line with values provided by the manufacturer (within 2 % of the declared value); therefore, this study refers to the manufacturers' values. As the copolymers have varying hydrophilicity and different physicochemical properties, the experiments were designed to highlight differences in polymer affinity for the drugs. A diffusion model for thin films was developed using time-resolved UV–Vis data, and the predicted diffusivity and partition coefficient were compared with drug release data.

3.1. Solubility study

HCT and CAF are stated by Ph. Eur. (EDQM, 2023) to be very slightly soluble and sparingly soluble in water, respectively. In this study, the solubility of HCT and CAF was determined to be 0.69 ± 0.03 mg/mL and 21.7 ± 0.3 mg/mL at pH 7.0, respectively, which are in good agreement with the literature (PubChem) (Table 1). According to the literature, CAF is classified as a Biopharmaceutics Classification System (BCS) class I drug, and HCT is a BCS class IV drug (Jain et al., 2022; Ruponen et al., 2020). The solubility values were used further to support the observations in the diffusivity and release studies.

3.2. Intrinsic viscosity, viscosity of the formulations, and critical overlap concentration

Intrinsic viscosity and c* for polymer solutions were obtained to gain information about the polymers, facilitating the understanding of the experimental system. The results in Table 2 show that the intrinsic viscosity of polymers increased with increasing VA proportion. Copolymers with more hydrophilic VA groups are more likely to form hydrogen bonds with water, which theoretically should expand their polymer coil size, leading to higher intrinsic viscosity (Kulicke & Clasen, 2004).

The theoretical transition from a dilute to a semi-dilute regime in a polymer solution is assumed to occur at c*. For polymer concentrations below c*, in the dilute regime, the polymer chains behave independently, while at c* the polymer coils start to interpenetrate, and intermolecular interactions begin to develop (Venkatesh et al., 2023). As c* is inversely related to the intrinsic viscosity, the c* values showed an opposite trend, i.e., decreasing with increased VA proportion. It should be noted that the most hydrophobic solutions, PVA35 and PVA50, were slightly turbid, suggesting that the polymer was not fully dissolved in mQ water, which might have affected the results.

In the diffusivity setup, a 5 % w/v polymer solution in water was injected. As seen in Table 2, the c* values range from 3.7 % to 25.3 %. For the polymer solutions to be in the semi-dilute regime, the polymer concentration should be larger than c*, meaning that in our systems, the two with the highest VA content are in the semi-dilute regime, whereas the others are not. The term 'polymer solution' in this paper will refer to a colloidal solution formed by dispersing the polymer in aqueous media.

The viscosity of the polymer solutions with the drugs (50 μg/mL drug and 50 mg/mL polymer in mQ water) varied depending on the type of copolymer, and they were shown to increase in this order: PVA35 < PVA50 < PVA88 < PVA74 < PVA98 (Table 2). The results align with previously determined viscosities of these polymers in higher concentrations, except PVA74, which was more viscous than PVA98 in our previous work (Korelc et al., 2024). This order was expected since more hydrophilic polymers (e.g., PVA98) were expected to dissolve and expand more in water, resulting in higher viscosity compared to hydrophobic copolymers (e.g., PVA35) with a higher acetate proportion that expands less. PVA88 did not fully follow the trend, suggesting that additional mechanisms may have been involved. These aqueous samples of PVA35 and PVA50 were also turbid as they did not fully dissolve in water, and potential phase separation might have resulted in a lower viscosity. The formulations with HCT and CAF had comparable viscosities for a given type of copolymer but displayed higher viscosities of PVA74 and PVA98 copolymer with HCT compared to CAF. This may imply different drug-polymer interactions for the two drugs. The viscosity of the polymer solution is an important factor in diffusivity

Table 2
Intrinsic viscosity (η), critical overlap concentration (c*) for copolymers, and viscosity of polymers (50 mg/mL) with HCT and CAF (50 μg/mL), respectively, presented as average ± standard deviation (n = 3).

Copolymer	η (mL/g)	c* (%)	Viscosity with HCT (mPa × s)	Viscosity with CAF (mPa × s)
PVA35	5.1 ± 0.3*	24.1 ± 1.2*	1.36 ± 0.04*	1.32 ± 0.04*
PVA50	6.8 ± 0.5*	18.1 ± 1.3*	1.75 ± 0.03*	1.81 ± 0.07*
PVA74	23.4 ± 1.3	5.2 ± 0.3	4.67 ± 0.07	4.53 ± 0.03
PVA88	30.3 ± 1.0	4.0 ± 0.1	4.03 ± 0.03	3.95 ± 0.04
PVA98	32.6 ± 0.3	3.7 ± 0.0	5.03 ± 0.26	4.65 ± 0.14

* The solutions were slightly turbid.

studies, as by the Stokes-Einstein equation, the drug is expected to diffuse slower from a more viscous solution than from a less viscous one (Falavigna et al., 2020; Hedaya, 2007).

3.3. Diffusion and partition investigation

Diffusion of small molecules in polymers and gels has been previously studied for decades by gravimetry, membrane permeation, fluorescence, and dynamic light scattering, resulting in a better understanding of the controlled release of drugs from polymeric carrier systems (Masaro & Zhu, 1999). In this paper, we propose to use localized UV–Vis spectroscopy to determine the drug absorbance as a function of time and, from that, estimate the diffusion coefficient for the drug and the interactions between the drug and polymer molecules, described by the partition constant. Pure polymer solutions were injected into the bottom of the cuvette, and UV–Vis spectra were recorded at 1.1 cm from the bottom to minimize the potential influence of polymer diffusion. The polymer solutions caused scattering, visible in the spectra as an increase in absorbance values of up to 0.02 after 20 h, while the absorbance values for diffusivity experiments with the drug in the polymer solution were approx. 10-fold (or more) higher (Supplementary material, Fig. S2). This indicates that the UV–Vis data were recorded at a sufficient distance from the bottom of the cuvette to avoid interference with the absorbance of the drug molecules. Notably, the scattering contributions to the UV–Vis spectra were highest for PVA35 and PVA88, lowest for PVA74, and showed no consistent trend among the copolymers with varying monomer ratios. In addition, the error between the two replicates tested was lower than 5 % (4.8 %) (Supplementary material, Fig. S3), indicating that the method can be considered reliable.

It should be noted that the absorbance of PVA35 during the diffusivity experiment began to increase after 13.3 h (Supplementary material, Fig. S2). Consequently, wavelength scans at different time points were conducted on pure PVA35 and HCT-PVA35 samples during the diffusivity experiments. Initially, the absorbance at 273 nm increased slowly with time for both samples (Supplementary material, Fig. S4). In the sample containing HCT, the peak at 273 nm was visible and could be clearly differentiated from the baseline, which made it possible to perform the subtractions.

HCT is UV-sensitive and prone to degradation when exposed to UV light for extended periods (Gumieniczek et al., 2018). Therefore, its stability under UV light was studied under the same conditions as the diffusivity experiments, and no HCT degradation was observed throughout the entire experiment (See Supplementary material, Fig. S5). Additionally, all formulations were exposed to the same environment, allowing for a relative comparison between samples containing HCT.

Fig. 4a and b show the concentration of HCT and CAF, respectively, at position X_1 as a function of time (black) and model prediction (red). A good agreement can be seen between the experimental data and model prediction. Through this fitting, it was possible to calculate the empirical reference diffusivities of PBS for both HCT ($7.8*10^{-6}$ cm^2/s; r_s 2.82 Å) and CAF ($7.7*10^{-6}$ cm^2/s; r_s 2.80 Å). Taking as reference the diffusivity of calcium ions in the water ($13.1*10^{-6}$ cm^2/s; r_s 1.5 Å) (Ribeiro et al.,

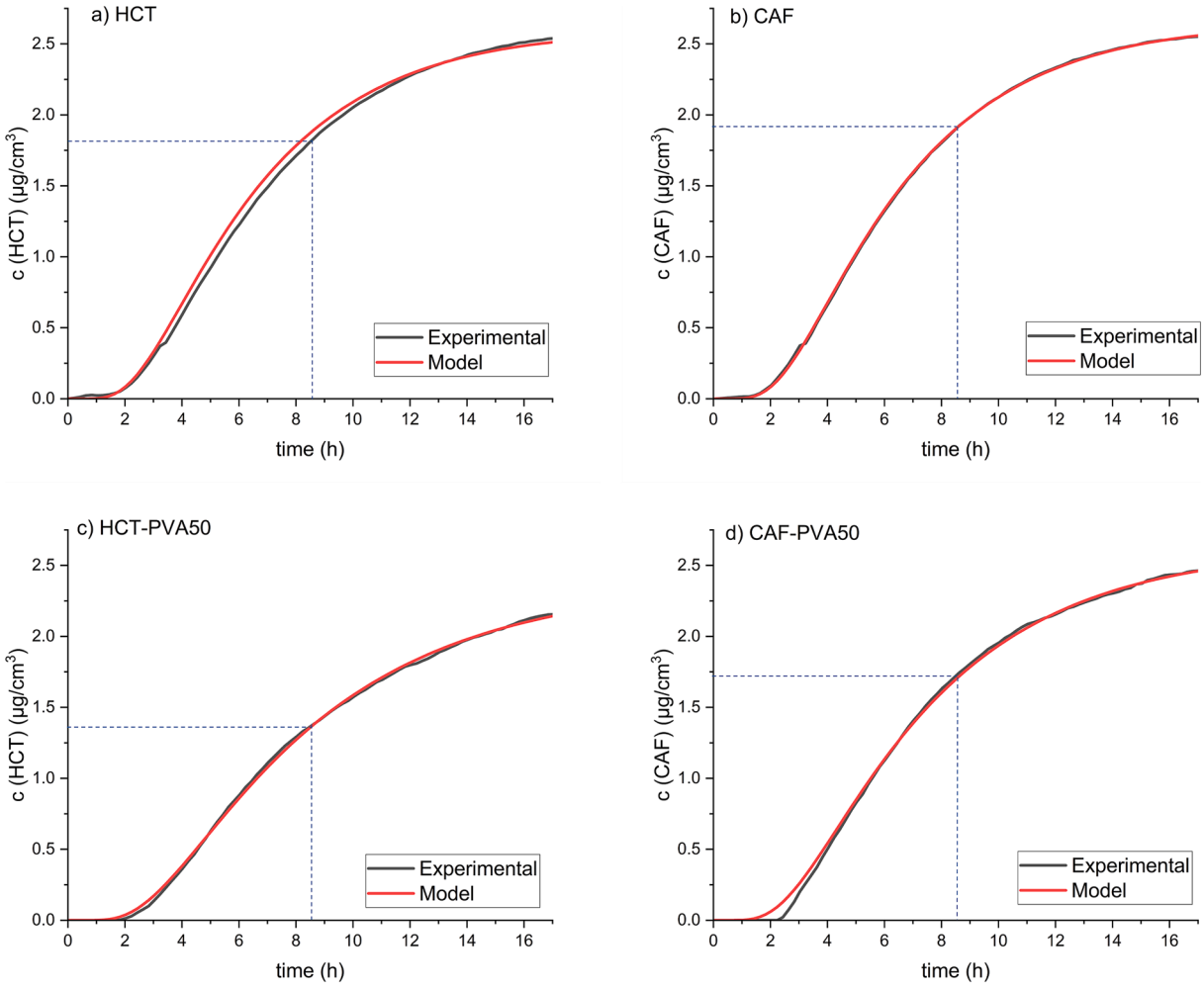

Fig. 4. Concentration profiles obtained from diffusivity measurements of a) HCT in PBS, b) CAF in PBS, c) HCT in PVA50 polymer solution in water, and d) CAF in PVA50 polymer solution in water. The experimental values are plotted against the fitted curve (model).

2008), the measured diffusivity values for CAF and HCT in water can be considered realistic.

In comparison, Fig. 4c and d show the experimental data where the absorbance from the polymer is subtracted, and the fittings for the diffusion of HCT and CAF from the polymer solution (PVA50). The statistical reliability of the model best fitting was proved by the F-test ($P > 0.4$ with a threshold set at 0.05). The presence of the polymer is expected to decrease the diffusion coefficient (García-Aparicio et al., 2012). Thus, for preliminary analysis of the effect of the polymer on drug transport, the experimental curves in Fig. 4 were compared. This is meaningful since the initial concentrations of the drugs and the drug-polymer mixtures were equal. Consequently, it is possible to directly compare the experimentally determined concentrations of the drugs at 1.1 cm from the bottom of the cuvette at a selected time to get an indication of the net transport of the drugs (see dashed lines in Fig. 4). When comparing the diffusion profiles of the pure drug and drug-PVA50, the reduction in drug concentration after 8.5 h was more pronounced for HCT than for CAF, suggesting HCT interacts with the polymer to a greater extent than CAF. To further investigate this, the mathematical model was fitted to experimental data for both drugs and for the different solutions considered (Fig. 5), always getting a positive F-test ($P > 0.4$). Model fitting parameters (D_{eff} and $K_{m/w}$) have been reported in Table 3.

Fig. 5 displays the diffusion curves of CAF and HCT from all the polymer solutions. The concentration of CAF increased over time and remained similar across all copolymers, indicating minimal dependence on the specific PVA/PVAc composition. Additionally, the CAF diffusion curves were comparable to the reference (50 μg/mL CAF in PBS), suggesting that the presence of the polymer does not significantly affect the diffusive transport of CAF. Similarly, the HCT-PVA98 concentration increase followed a similar time dependence as the reference (50 μg/mL HCT in PBS), suggesting that the most hydrophilic copolymer, PVA98, does not retain HCT or delay its diffusion. It can also be observed that the concentration of HCT increased more slowly in copolymers with the highest proportion of acetate groups (PVA35 and PVA50). It is well-known from the literature that increased viscosity decreases the diffusion coefficient (Tyrell, 1981). In this study, we observed that despite PVA35 and PVA50 being less viscous than the more hydrophilic copolymers, the diffusive transport of HCT was slower from these polymer solutions than those with higher viscosity. Thus, this shows that the experimental data needs another explanation. Here, we suggest that drug-polymer interactions can slow down the diffusive transport of HCT. The literature indicates that such hydrophobic interactions can influence drug transport (Varshosaz & Falamarzian, 2001).

Table 3 shows the estimated partitioning coefficients ($K_{m/w}$) for HCT and CAF. This value represents the distribution of each drug between the polymer solution and the acceptor media (i.e., the water phase) at thermodynamic equilibrium, reflecting the interactions between the drugs and the polymers. Estimations for HCT provided the highest $K_{m/w}$ value for the copolymer with the most hydrophobic character, PVA35, aligning with the observations in Fig. 5. Furthermore, $K_{m/w}$ values for HCT decreased with an increasing proportion of the hydrophilic VA group. This results in the lowest calculated $K_{m/w}$ value for the copolymer PVA98, approaching a $K_{m/w}$ value closer to 1, suggesting that the drug is likely to distribute more evenly between the polymer solution and the aqueous media, indicating a much smaller affinity towards the polymer. Based on these results, it can be speculated that the partition mechanism in the studied copolymer systems effectively explains the net diffusive transport of a BCS class IV drug.

Table 3
Partitioning coefficient ($K_{m/w}$) and effective diffusion coefficient (D_{eff}) for HCT and CAF with respect to the copolymers, determined by model (Eq. (4) and Eq. (6) fitting to experimental data (see Fig. 4 and Fig. 5). Model fitting was performed by fixing the nominal (injected) concentration (50 μg/mL) and setting the HCT and CAF diffusion coefficient in PBS (D_w) ($D_{HCT} = 7.8*10^{-6}$ cm^2/s; $D_{CAF} = 7.7*10^{-6}$ cm^2/s). Model fitting statistical reliability was proved by the F-test ($P > 0.4$ with a threshold set at 0.05).

	$K_{m/w}$ (HCT)	D_{eff} (HCT) (cm^2/s)	D_{eff} (CAF) (cm^2/s)	$K_{m/w}$ (CAF)
PVA35	6.61	$1.2*10^{-6}$	$5.0*10^{-6}$	1.29
PVA50	6.13	$0.8*10^{-6}$	$4.1*10^{-6}$	1.38
PVA74	2.47	$4.0*10^{-6}$	$5.7*10^{-6}$	1.36
PVA88	1.64	$4.5*10^{-6}$	$1.7*10^{-6}$	1.04
PVA98	1.54	$4.2*10^{-6}$	$1.5*10^{-6}$	0.58

Fig. 5 indicates that CAF exhibited low affinity towards the PVA/PVAc copolymers, leading to the expectation that the fitted $K_{m/w}$ values for CAF would be similar across the different copolymers. However, as seen in Table 3, the more hydrophobic copolymers tended to retain CAF to some extent, as their $K_{m/w}$ was lower than for the more hydrophilic polymers. Thus, CAF may form hydrophobic interactions with VAc chains, but to a smaller extent than HCT. CAF appears to interact minimally with the more hydrophilic polymers, indicating a low potential affinity between the drug and the polymer. Consequently, the net diffusive transport of CAF is nearly as fast as it would be without any polymer present. This can only be the case when the polymer concentration is in the dilute regime, preventing the polymer chains from significantly hindering CAF diffusion.

Table 3 also shows the fitted diffusion coefficient (D_{eff}) for HCT and CAF for various copolymers. This parameter explains how the drug

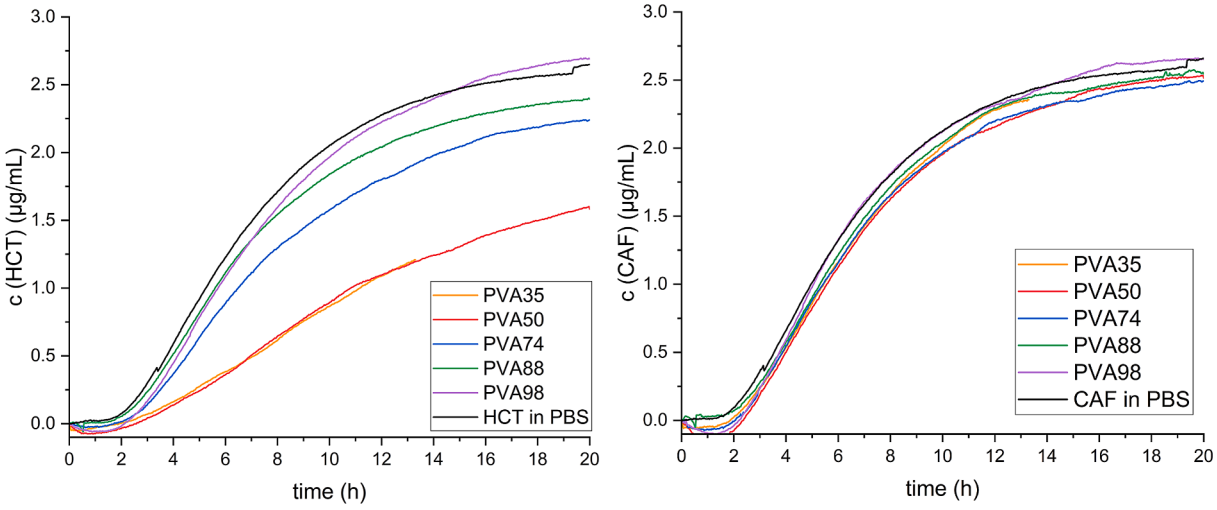

Fig. 5. HCT (left) and CAF (right) concentration profile over time obtained from the diffusivity measurements. The polymer background is subtracted.

molecules move within the polymer solution. The D_{eff} for HCT is higher for more hydrophilic copolymers, i.e. PVA74, PVA88, and PVA98. These results align with observations from Fig. 5 and indicate that when the drug molecules are surrounded by the presence of polymers with a larger proportion of VAc groups, they diffuse through the polymer media slower, likely due to hydrophobic drug-polymer interactions. On the other hand, CAF shows the opposite trend. D_{eff} is lower for CAF in the case of the more hydrophilic polymers, i.e. PVA88 and PVA98. This effect may be observed due to the formation of hydrogen bonds between CAF and hydroxyl groups of the VA chains of the polymer. Even though CAF is surrounded by the aqueous environment and is likely to form hydrogen bonds with water molecules, it is likely that it is more thermodynamically favorable to interact with the polymer. D_{eff} for CAF-PVA74 would be expected to be lower than CAF-PVA50, suggesting that the model provides approximate values, and should therefore not be seen as an absolute value.

The drug-polymer interactions discussed would ideally have been confirmed by other relevant and well-established methods. The authors have used several methods for this purpose, and some of them are presented in the previous paper (Korelc et al., 2024). However, due to poor aqueous solubility of HCT, the high melting point of HCT leading to degradation of the polymer, and the low ratio of drug to polymer (5/400), conventional methods, such as Fourier-transform infrared spectroscopy (FTIR), differential scanning calorimetry (DSC) or X-ray powder diffraction (XRPD) turned out to be not suitable for these systems.

3.4. Correlation between diffusivity data and drug release

The release experiment revealed differences between copolymers and between the two chemically different drugs. The drug release from HCT-containing films was determined in a previous study (Korelc et al., 2024) and is shown in Fig. 6a. Fig. 6b shows the CAF release profile from the films. The release curves for PVA88 and PVA98 were similar for both CAF and HCT, exemplified by the drug release rates during the first 30 min for these two copolymers not being significantly different. It would be expected that large differences in solubility between these drugs should be the controlling parameter for drug release, even for film formulations with the most hydrophilic copolymers. However, the results clearly show that this is not the case. This might be explained by both drugs having time to dissolve in the hydrated film, (i.e., with the polymers in the semi-dilute regime), possibly due to the film preparation process inducing solid-state morphologies, like solid solutions/dispersions, that dissolve quickly. Once dissolved, the drug is transported through the entangled polymer solution via diffusion, and during this process, interactions between the drug and polymer can occur.

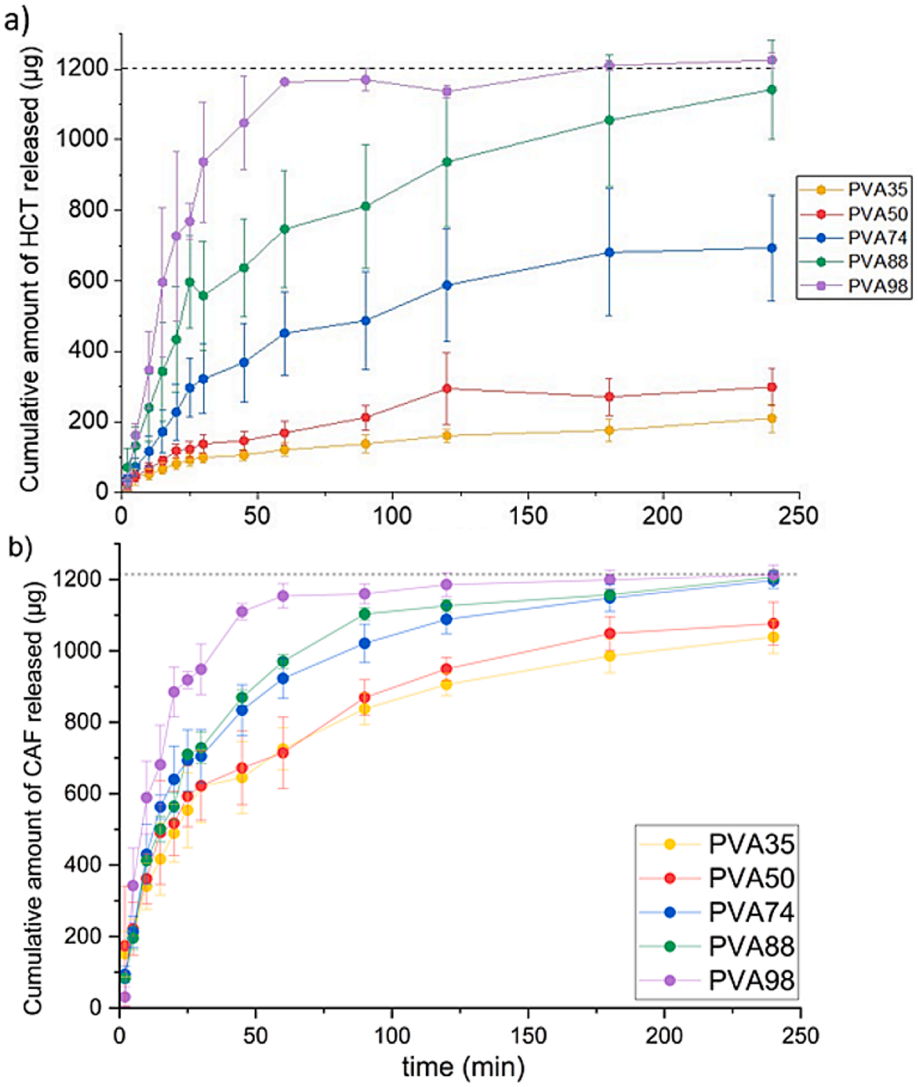

Fig. 6. Cumulative amount of a) HCT (reproduced from Korelc et al., 2024) and b) CAF release from the films, normalized per a 100 mg film piece. The values are presented as average ± standard deviation (n = 3).

However, in this case, the system does not gain free energy from such interactions between hydrophilic polymers and hydrophilic drugs. In contrast, for the same drugs with more hydrophobic polymers (PVA35 and PVA50), it was observed that at the end of the experiment (4 h), 12–27 % of HCT was released, while this value for CAF was 78–91 %. The slower release of the more hydrophobic HCT could be attributed to the system gaining free energy from interactions between hydrophobic regions within the polymer and the HCT molecules. Another factor influencing the drug release rate can be the behavior of films in the release media. It was observed that the films exhibited different disintegration and erosion behavior depending on the hydrophilicity of the copolymer. The films made of more hydrophobic polymers, PVA35 and PVA50, curled up into small polymer lumps after approximately 10–15 min and tended to stick to the bottom surface as small polymer lumps. This can be attributed to their poor solubility in PBS, and consequently a slower drug release rate was detected compared to the copolymers that were better soluble in the dissolution media. On the other hand, the films made of more hydrophilic copolymers started to disintegrate after approximately 20 min, and after 30 min only smaller fragments could be observed. A higher contact area with the release media might have contributed to the faster drug release.

The diffusivity and drug release rate were combined to understand if the diffusivity method can be applied to predict the drug release from the thin films. As the films were relatively thin, with a thickness of up to 450 μm (Korelc et al., 2024), the hydration of such thin systems would be relatively fast, leading to a fast formation of the swollen structure with no solid core – this allows for correlation of release from a solid form with the polymer solution. Fig. 7 shows the correlation between the calculated efficient diffusion coefficient $1/K_{m/w}$ and the drug released after 20 min of the study. This time point was chosen as the amount of drug released clearly differed between formulations. Fig. 7 indicates that the amount of drug released can be correlated to the calculated efficient diffusion constant, and the fitting had a relatively good correlation coefficient ($r = 0.930$), showing that the diffusion parameters estimate differences seen in the release studies. The estimated $K_{m/w}$ (Table 3) were rather similar and close to 1 for CAF, which explains why the CAF formulations are located close to each other in the correlation plot (Fig. 7). As discussed above, the more water-soluble drug CAF is well dissolved in the PBS and show lower affinity towards the polymer. Both drugs were included in the fitting as they have a similar radius and similar diffusion coefficient, therefore their effective diffusion coefficient is expected to be similar. Despite the fact that the figure shows $1/K_{m/w}$, D_{eff}/D_m can be considered equivalent (see Eq. (5). Even though the correlation was observed, the differences in the release profile were pronounced for CAF, which the diffusion method did not account for. Therefore, this can be seen as a screening method that can facilitate the choice of drug-polymer combinations and the formulation process, but it cannot fully replace necessary release experiments that provide more realistic/accurate data, as the model does not account for hydration and swelling of the film, that occur when a solid film gets into contact with aqueous media. These factors should be considered and determined, as they can critically influence the properties and behavior of the drug in the formulation. However, the focus of this work was to present a quick, easy, and inexpensive method that could aid with screening different drug-polymer combinations and observing for potential differences among them, and this method appeared suitable for this purpose.

4. Conclusion

In this work, we hypothesized that drug release from polymeric thin films could be estimated by looking at drug diffusivity in diluted drug-polymer solutions. To test this hypothesis, we applied the UV–Vis localized spectroscopic method introduced by di Cagno et al. (2018) and further optimized by Falavigna *et al.* (2019). We varied the polymers' hydrophilicity by using PVA/PVAc copolymers with vinyl alcohol ratios ranging from 35 % to 98 %, and we examined the hydrophilicity

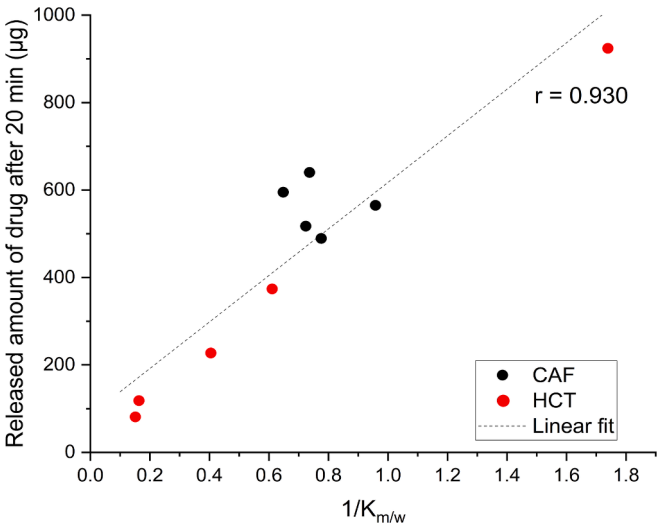

Fig. 7. Correlation between the cumulative amount of drug released from films after 20 min of the experiment (HCT and CAF) and calculated efficient diffusion coefficient, here shown as $1/K_{m/w}$.

dimensions of the drugs by using HCT and CAF with a solubility ratio of 1:30. The UV–Vis localized spectroscopic method resulted to be suitable for the purpose, showing a positive correlation between diffusional data and classical film release rates. Moreover, it was found that the interactions were strongest for the most hydrophobic drug/polymer formulations and weakest for the most hydrophilic formulations. Our findings demonstrate that combining diffusion and release experiments provides a deeper understanding of the drug release mechanism. Therefore, this method can be seen as a promising, quick, and inexpensive tool for developing polymer-based thin films.

CRediT authorship contribution statement

Karin Korelc: Writing – original draft, Visualization, Methodology, Investigation, Formal analysis, Data curation, Conceptualization. **Martina M. Tzanova:** Writing – review & editing, Methodology, Conceptualization. **Anette Larsson:** Writing – review & editing, Supervision, Data curation, Conceptualization. **Mario Grassi:** Writing – review & editing, Formal analysis, Data curation. **Massimiliano Pio Di Cagno:** Writing – review & editing, Supervision, Project administration, Methodology, Formal analysis, Data curation, Conceptualization. **Ingunn Tho:** Writing – review & editing, Supervision, Resources, Project administration, Methodology, Funding acquisition, Data curation, Conceptualization.

Declaration of competing interest

The authors declare that they have no known competing financial interests or personal relationships that could have appeared to influence the work reported in this paper.

Acknowledgements

The authors would like to acknowledge Kuraray Poval™ for providing PVA/PVAc copolymers and thank Bjarke Strøm Larsen for valuable discussions, as well as for contacting the company and providing us with the mentioned copolymers.

Appendix A. Supplementary material

Supplementary data to this article can be found online at https://doi.org/10.1016/j.ijpharm.2025.125491.

Data availability

Data will be made available on request.

References

Adrover, A., Nobili, M., 2015. Release kinetics from oral thin films: Theory and experiments. *Chem. Eng. Res. Des.* 98, 188–201. https://doi.org/10.1016/j.cherd.2015.04.016.

Adrover, A., Varani, G., Paolicelli, P., Petralito, S., Di Muzio, L., Casadei, M.A., Tho, I., 2018. Experimental and modeling study of drug release from HPMC-based erodible oral thin films. *Pharmaceutics* 10 (4), 222. https://doi.org/10.3390/pharmaceutics10040222.

Ahmad Bhawani, S., Fong, S.S., Mohamad Ibrahim, M.N., 2015. Spectrophotometric analysis of caffeine. *Int. J. Anal. Chem.* 2015, 170239. https://doi.org/10.1155/2015/170239.

Amsden, B.G., 2022. Hydrogel mesh size and its impact on predictions of mathematical models of the solute diffusion coefficient. *Macromolecules* 55 (18), 8399–8408. https://doi.org/10.1021/acs.macromol.2c01443.

Atanase, L.I., Riess, G., 2010. Poly(vinyl alcohol-co-vinyl acetate) complex formation with anionic surfactants particle size of nanogels and their disaggregation with sodium dodecyl sulfate. *Colloids Surf. A Physicochem. Eng. Asp.* 355 (1–3), 29–36. https://doi.org/10.1016/j.colsurfa.2009.11.024.

Benet, L.Z., Broccatelli, F., Oprea, T.I., 2011. BDDCS applied to over 900 drugs. *AAPS J.* 13 (4), 519–547. https://doi.org/10.1208/s12248-011-9290-9.

Colombo, P., 1993. Swelling-controlled release in hydrogel matrices for oral route. *Adv. Drug Deliv. Rev.* 11 (1–2), 37–57. https://doi.org/10.1016/0169-409X(93)90026-Z.

Desmedt, B., Courselle, P., De Beer, J.O., Rogiers, V., Deconinck, E., De Paepe, K., 2015. In vitro dermal absorption: sample application and seal quality in a franz diffusion cell system. *Skin Pharmacol. Physiol.* 28 (5), 245–249. https://doi.org/10.1159/000375321.

Di Cagno, M.P., Clarelli, F., Vabenø, J., Lesley, C., Rahman, S.D., Cauzzo, J., Franceschinis, E., Realdon, N., Stein, P.C., 2018. Experimental determination of drug diffusion coefficients in unstirred aqueous environments by temporally resolved concentration measurements. *Mol. Pharm.* 15 (4), 1488–1494. https://doi.org/10.1021/acs.molpharmaceut.7b01053.

Di Cagno, M.P., Stein, P.C., 2019. Studying the effect of solubilizing agents on drug diffusion through the unstirred water layer (UWL) by localized spectroscopy. *Eur. J. Pharm. Biopharm.* 139, 205–212. https://doi.org/10.1016/j.ejpb.2019.04.005.

Falavigna, M., Stein, P.C., Flaten, G.E., Di Cagno, M.P., 2020. Impact of mucin on drug diffusion: Development of a straightforward in vitro method for the determination of drug diffusivity in the presence of mucin. *Pharmaceutics* 12 (2), 168. https://doi.org/10.3390/pharmaceutics12020168.

Flory, P.J., 1953. *Principles of Polymer Chemistry*. Cornell University Press.

García-Aparicio, C., Quijada-Garrido, I., Garrido, L., 2012. Diffusion of small molecules in a chitosan/water gel determined by proton localized NMR spectroscopy. *J. Colloid Interf. Sci.* 368 (1), 14–20. https://doi.org/10.1016/j.jcis.2011.11.028.

Grassi, M., Grassi, G., Lapasin, R., Colombo, I., 2006. *Understanding Drug Release and Absorption Mechanisms: A Physical and Mathematical Approach*. CRC Press.

Gumieniczek, A., Galeza, J., Mroczek, T., Wojtanowski, K., Lipska, K., Pietras, R., 2018. Kinetics and characterization of degradation products of dihydralazine and hydrochlorothiazide in binary mixture by HPLC-UV, LC-DAD and LC–MS methods. *Chromatographia* 81 (8), 1147–1162. https://doi.org/10.1007/s10337-018-3555-8.

Hedaya, M.A., 2007. *Basic Pharmacokinetics*. CRC Press.

Karki, S., Kim, H., Na, S.J., Shin, D., Jo, K., Lee, J., 2016. Thin films as an emerging platform for drug delivery. *Asian J. Pharm. Sci.* 11 (5), 559–574. https://doi.org/10.1016/j.ajps.2016.05.004.

Korelc, K., Larsen, B.S., Heintze, A.-L., Henrik-Klemens, Å., Karlsson, J., Larsson, A., Tho, I., 2024. Towards personalized drug delivery via semi-solid extrusion: exploring poly(vinyl alcohol-co-vinyl acetate) copolymers for hydrochlorothiazide-loaded films. *Eur. J. Pharm. Sci.* 192, 106645. https://doi.org/10.1016/j.ejps.2023.106645.

Kulicke, W.-M., Clasen, C., 2004. Determination of the polymer coil dimensions from the intrinsic viscosity. In: *Viscosimetry of Polymers and Polyelectrolytes*. Springer, Berlin, Heidelberg, pp. 91–94.

Masaro, L., Zhu, X.X., 1999. Physical models of diffusion for polymer solutions, gels and solids. *Prog. Polym. Sci.* 24 (5), 731–775. https://doi.org/10.1016/S0079-6700(99)00016-7.

Medarević, D., Djuriš, J., Barmpalexis, P., Kachrimanis, K., Ibrić, S., 2019. Analytical and computational methods for the estimation of drug-polymer solubility and miscibility in solid dispersions development. *Pharmaceutics* 11 (8), 372. https://doi.org/10.3390/pharmaceutics11080372.

Jain, M.H.K., Hou, H.H., Siegel, R.A., 2022. An artificial gut/absorption simulator: description, modeling, and validation using caffeine. *AAPS J.* 24 (87). https://doi.org/10.1208/s12248-022-00721-1.

Patankar, S.V., 1980. *Numerical Heat Transfer and Fluid Flow*. Hemisphere Publishing Corporation.

Ph. Eur. 11.2. (2023). EDQM, Council of Europe.

Pulsoni, I., Lubda, M., Aiello, M., Fedi, A., Marzagalli, M., von Hagen, J., Scaglione, S., 2022. Comparison between franz diffusion cell and a novel micro-physiological system for in vitro penetration assay using different skin models. *SLAS Technol.* 27 (3), 161–171. https://doi.org/10.1016/j.slast.2021.12.006.

Puttipipatkhachorn, S., Nunthanid, J., Yamamoto, K., Peck, G.E., 2001. Drug physical state and drug-polymer interaction on drug release from chitosan matrix films. *J. Control. Release* 75 (1–2), 143–153. https://doi.org/10.1016/S0168-3659(01)00389-3.

PubChem (n.d.). Retrieved February 12, 2024, from https://pubchem.ncbi.nlm.nih.gov/.

Ribeiro, A.C.F., Barros, M.C.F., Teles, A.S.N., Valente, A.J.M., Lobo, V.M.M., Sobral, A.J.F.N., Esteso, M.A., 2008. Diffusion coefficients and electrical conductivities for calcium chloride aqueous solutions at 298.15 K and 310.15 K. *Electrochim. Acta* 54 (2), 192–196. https://doi.org/10.1016/j.electacta.2008.08.011.

Ruponen, M., Rusanen, H., Laitinen, R., 2020. Dissolution and permeability properties of co-amorphous formulations of hydrochlorothiazide. *J. Pharm. Sci.* 109 (7), 2252–2261. https://doi.org/10.1016/j.xphs.2020.04.008.

Tyrell, H., 1981. Diffusion and viscosity in the liquid phase. *Sci. Prog.* 67 (266), 271–293.

Tzanova, M.M., Moretti, F., Grassi, G., Stein, P.C., Hiorth, M., Abrami, M., Grassi, M., di Cagno, M.P., 2022. Modelling drug diffusion through unstirred water layers allows real-time quantification of free/loaded drug fractions and release kinetics from colloidal-based formulations. *Eur. J. Pharm. Biopharm.* 178, 168–178. https://doi.org/10.1016/j.ejpb.2022.08.009.

Varshosaz, J., Falamarzian, M., 2001. Drug diffusion mechanism through pH-sensitive hydrophobic/polyelectrolyte hydrogel membranes. *Eur. J. Pharm. Biopharm.* 51 (3), 235–240. https://doi.org/10.1016/S0939-6411(01)00126-6.

Venkatesh, R., Zheng, Y., Liu, A.L., Zhao, H., Silva, C., Takacs, C.J., Grover, M.A., Meredith, J.C., Reichmanis, E., 2023. Overlap concentration generates optimum device performance for DPP-based conjugated polymers. *Org. Electron.* 117, 106779. https://doi.org/10.1016/j.orgel.2023.106779.